Supplementary information

A flame-retardant polyimide interlayer with polysulfide lithium traps and fast redox conversion towards safety and high sulfur utilization Li-S batteries

Zhiyu Zhou[ab], Zexiang Chen[ab], Yang Zhao[ab], Huifang Lv[ab], Hualiang Wei[ab], Bingbing Chen[c], Zengjie Gu[d], and Yan Wang[ab]**

[a]School of Optoelectronic Science and Engineering, University of Electronic Science and Technology of China, 611731 Chengdu, China

[b]Sichuan Province Key Laboratory of Display Science and Technology, Jianshe North Road 4, 610054 Chengdu, China

[c]Department of Energy Science and Engineering, Nanjing Tech University, Nanjing, 210009, China

[d]Science and Technology on Vacuum Technology and Physics Laboratory, Lanzhou Institute of Physics, No.108, Yanxing Road, 730000 Lanzhou, China

E-mail: zxchen@uestc.edu.cn (Zexiang Chen); wangyan127@uestc.edu.cn (Yan Wang)

DFT computations

All first-principle calculations were based on the Vienna Ab Initio Package (VASP)[1, 2] within the gene ximation (GGA) using the Perdew-Burke-Ernzerhof (PBE) formulation[3]. Ionic cores were depicted with projected augmented wave (PAW) potentials[4, 5], and the valence electrons were taken into account using a plane wave basis set (400 eV kinetic energy cutoff). Partial occupancies of the Kohn-Sham orbitals were allowed using the Gaussian smearing method and a width of 0.05 eV. The electronic energy was regarded as self-consistent when the energy change was lower than 10^{-7} eV. A geometry optimization was considered convergent when the energy change was less than 10^{-6} eV. Grimme's DFT-D3 methodology[6] was used to describe the dispersion interactions among all atoms in the PI monomer and corresponding adsorption models.

The equilibrium lattice constant of the PI monomer in the *x* direction was optimized when setting $y = z = 15$ Å and using a 1 × 1 × 1 Monkhorst-Pack k-point grid for Brillouin zone sampling. The optimized lattice constant was found to be $x = 22.20$ Å. Full relaxation was permitted for all atoms during structure optimization. The adsorption energy (E_{ads}) of the adsorbate was specified as Equation S1:

$$E_{ads} = E_{LiS/polyimide} - E_{polyimide} - E_{LiS} \quad \text{(S1)}$$

where $E_{LiS/polyimide}$, $E_{polyimide}$ and E_{LiS} are the energy of the adsorbate Li_2S_n (n = 1, 2, 4, 6) after being adsorbed on PI, the energy of pristine PI, and the energy of isolated Li_2S_n (n = 1, 2, 4, 6) molecules in a cubic periodic box with a side length of 20 Å and a 1 × 1 × 1 Monkhorst-Pack k-point grid for Brillouin zone sampling, respectively.

Table S1. Slope values obtained from linear fitting of the peak current (i_p) versus square root of the scan rate ($v^{0.5}$) plots shown in Fig. 4d–f.

Slope values of linear fitting lines [mA $(V/s)^{-1/2}$]			
Configuration	Peak I	Peak II	Peak III
Bare	310.80	182.66	241.52
With SS-PI interlayer	670.77	357.45	503.72
With Ni/SS-PI interlayer	1235.13	636.50	759.08

Table S2. Fitted Tafel slope values derived from the Tafel plots shown in Fi. 4g–i.

Values of fitted Tafel slopes [mV/dec]			
Configuration	2.16 V–2.34 V	2.37 V–2.46 V	2.01 V–2.07 V
Bare	198.1	67.7	126.2
With SS-PI interlayer	147.6	54.5	67.6
With Ni/SS-PI interlayer	117.2	32.6	27.9

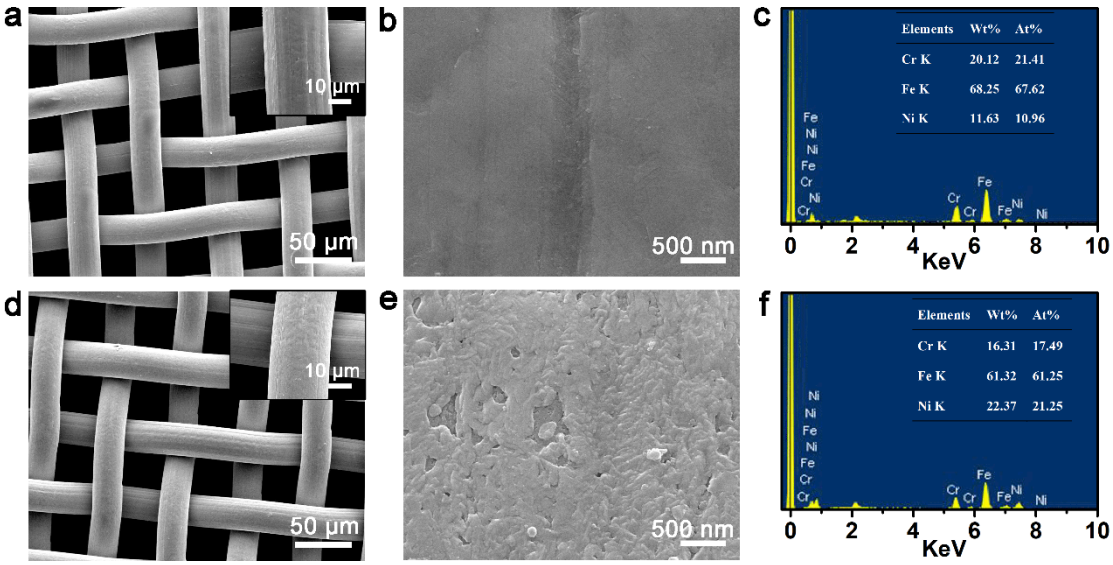

Fig. S1. SEM images of the unplated SS surface at (a) low and (b) high magnification. (c) EDS maps of the unplated SS surface. SEM images of the Ni-plated SS surface at (d) low and (e) high magnification. (f) EDS maps of the Ni/SS surface.

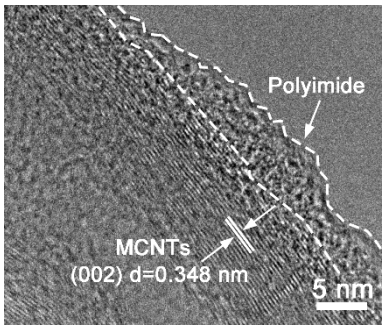

Fig. S2. TEM image of the PI/MCNT compounds at high magnification. Amorphous PI covers the surface of the MCNTs.

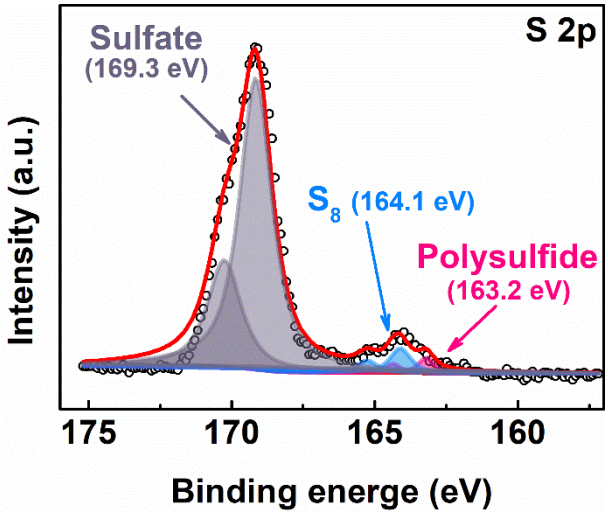

Fig. S3. S 2p XPS spectrum of the SS-PI interlayer after 50 cycles.

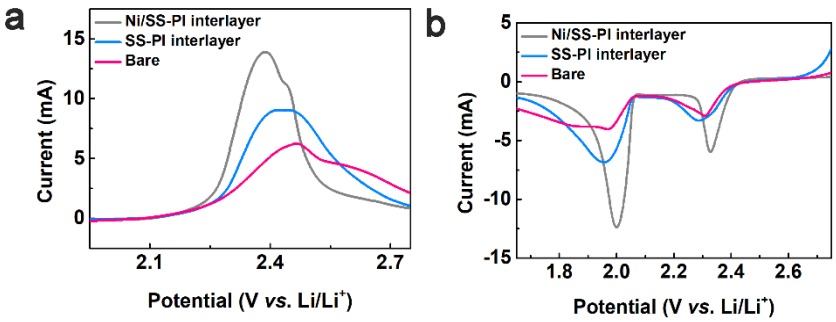

Fig. S4. LSV curves (obtained at a scan rate of 0.2 mV s^{-1}) for the (a) anodic peak corresponding to the oxidation of Li_2S to sulfur and (b) two cathodic peaks corresponding to the reduction of sulfur to Li_2S.

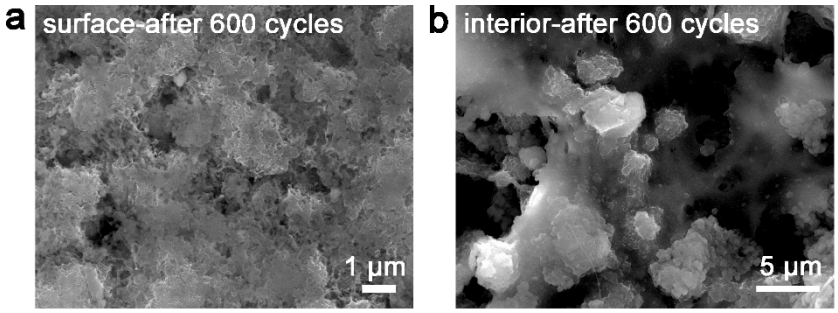

Fig. S5. SEM images of the a) surface and b) interior of Ni/SS-PI interlayer over 600 cycles at 0.5 C.

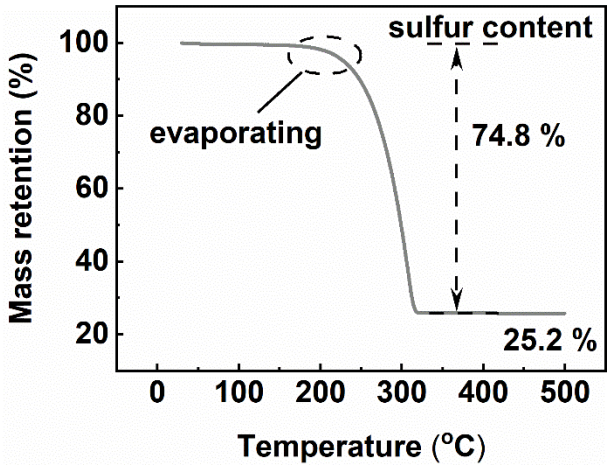

Fig. S6. TGA curve for the active material mixture consisting of sulfur, MCNTs and Super-P, which was used to prepare the cathode.

The sulfur content of the cathode is calculated based on TGA (Fig. S6). As it shown, the sulfur content is 74.8% by mass of the mixture of sulfur, MCNTs and Super-P. After the PVDF binder is added into the mixture to prepare the active material slurry, the sulfur content in cathode turns into 67.3% due to the additional 10% mass ratio of PVDF binder.

Video S1. Burning tests for Ni/SS gauze on a continuous flame.

Video S2. Burning tests for Ni/SS-PI interlayer on a continuous flame.

Supporting references

1. G. Kresse and J. Furthmüller, Efficiency of ab-initio total energy calculations for metals and semiconductors using a plane-wave basis set, *Comput. Mater. Sci.*, 1996, **6**, 15-50.
2. G. Kresse and J. Furthmüller, Efficient iterative schemes for ab initio total-energy calculations using a plane-wave basis set, *Phys. Rev. B*, 1996, **54**, 11169.
3. J. Perdew, K. Burke and M. Ernzerhof, Generalized gradient approximation made simple [Phys. Rev. Lett. 77, 3865 (1996)], *Phys. Rev. Lett.,* 1997, **78**.
4. G. Kresse and D. Joubert, From ultrasoft pseudopotentials to the projector augmented-wave method, *Phys. Rev. B*, 1999, **59**, 1758-1775.

5. P. Blöchl, Projector augmented-wave method, *Phys. Rev. B,* 1995, **50**, 17953-17979.
6. S. Grimme, J. Antony, S. Ehrlich, H. Krieg, A consistent and accurate ab initio parametrization of density functional dispersion correction (DFT-D) for the 94 elements H-Pu, *J. Chem. Phys.*, 2010, **132**, 154104.